Optics Communications 285 (2012) 1895–1899

Contents lists available at SciVerse ScienceDirect

Optics Communications

journal homepage: www.elsevier.com/locate/optcom

Emission enhancement ratio of the metal irradiated by femtosecond double-pulse laser

Jin Guo [a], Tingfeng Wang [a], Junfeng Shao [a], Tao Sun [a], Rui Wang [a], Anmin Chen [a,b,*], Zhan Hu [b], Mingxing Jin [b,*], Dajun Ding [b]

[a] State Key Laboratory of Laser Interaction with Matter, Changchun Institute of Optics, Fine Mechanics and Physics, Chinese Academy of Sciences, Changchun 130033, People's Republic of China
[b] Institute of Atomic and Molecular Physics, Jilin University, Changchun 130012, People's Republic of China

ARTICLE INFO

Article history:
Received 19 May 2011
Received in revised form 8 November 2011
Accepted 10 December 2011
Available online 22 December 2011

Keywords:
Emission enhancement
Two-temperature model
Double-pulse laser

ABSTRACT

A numerical solution of the two-temperature model has been performed up to the double-pulse femtosecond laser heated metal target. The two-temperature model is used to analyze the double-pulse laser with the following major conclusions. We confirm the distinctly different results on the single pulse and double pulse. The double-pulse laser heated lattice temperature is higher than the single pulse. Through the Boltzmann equation, we estimate the variation of the emission enhancement. At the same time, this experimental result is qualitatively similar to the theoretical result.

1. Introduction

Since the advent of the laser nearly 50 years ago, more and more attention of researchers has been paid to laser-induced breakdown spectroscopy (LIBS). LIBS operates by focusing the laser onto a small area at the surface of the specimen; when the laser is discharged it ablates a very small amount of material, in the range of nanograms to picograms, which generates a plasma plume. During data collection, typically after local thermodynamic equilibrium is established. In principle, LIBS can analyze any matter regardless of its physical state, be it solid, liquid or gas. Because all elements emit light of characteristic frequencies when excited to sufficiently high temperatures, LIBS can (in principle) detect all elements, limited only by the power of the laser as well as the sensitivity and wavelength range of the spectrograph and detector.

Recent developments in laser-induced breakdown spectroscopy (LIBS) have seen the introduction of double-pulsed laser systems. In the configuration the laser is fired twice on the same spot on the specimen with a pulse separation [1]. Depending on the pulse separation, the evolution of plasma is different from LIBS of the single pulse. For example, reducing nanoparticles in metal ablation plumes produced by two delayed short laser pulses [2], plume composition control in double pulse ultrafast laser ablation of metals [3], investigation of plumes produced by material ablation with two time-delayed femtosecond laser pulses [4], multidiagnostic analysis of ultrafast laser ablation of metals with pulse pair irradiation [5], and so on. In particular, the double-pulse (DP) technique in laser-induced breakdown spectroscopy can give higher luminosity of plasma in comparison with a single pulse (SP) of the same entire energy and thus improve the accuracy of measurements [6–9]. These results are based on three classes of mechanisms: it is possible that the fluorescence increases because more material is ablated from the surface by a double pulse as the result of a surface transformation induced by the first pulse; the enhancement may be caused by reheating of the plasma generated by the first pulse; hydrodynamic effects induced by the first pulse may affect the propagation of the laser beam and the expansion of the plume generated by the second pulse. These are just supposed analysis. It is essential to take the theoretical method into account the emission enhancement phenomena in metals.

In the present letter, the emission enhancement on the plasma from a copper surface under the double-pulse femtosecond laser is studied by means of a 1D two-temperature equation and Boltzmann equation. The motivation for doing this work is to develop a simple theoretical model for the double-pulse LIBS on the metal in order to better understand the mechanisms of the emission enhancement. At the same time, it presented an experimental study of the emission of the plasmas generated using both single-pulse and collinear double-pulse ablation copper in an effort to observe LIBS signal enhancement.

* Corresponding authors at: Institute of Atomic and Molecular Physics, Jilin University, Changchun 130012, People's Republic of China.
E-mail addresses: comeongoon@sohu.com (A. Chen), mxjin@jlu.edu.cn (M. Jin).

0030-4018/$ – see front matter © 2011 Elsevier B.V. All rights reserved.
doi:10.1016/j.optcom.2011.12.038

2. Mathematical model

The theoretical method to investigate the ultrashort laser–matter interaction is the well-known two-temperature model (TTM) [10]. The TTM describes the evolution of the temperature increase due to the absorption of a laser pulse within the solid and is applied to model physical phenomena like the energy transfer between electrons and lattice occurring during the target–laser interaction [11]. Therefore the expressions for the time evolution of the temperatures read [12,13]:

$$C_e\frac{\partial T_e}{\partial t}=\frac{\partial}{\partial x}\left(k_e\frac{\partial T_e}{\partial x}\right)-G(T_e-T_l)+S(x,t) \tag{1}$$

$$C_l\frac{\partial T_l}{\partial t}=G(T_e-T_l) \tag{2}$$

Where t is the delay time, x is the depth, C_e is the electron heat capacity, $C_l=3.5\times10^6 J/m^3K$ is the lattice heat capacity [14], k_e is the electron thermal conductivity, T_e is the electron temperature, T_l is the lattice temperature, G is the electron-lattice coupling factor [15,16], and S is the laser heat source. The heat source S can be modeled with a Gaussian temporal profile [17]:

$$S(x,t)=\sqrt{\frac{\beta}{\pi}}\frac{(1-R)I}{t_p\alpha}\exp\left[-\frac{x}{\alpha}-\beta\left(\frac{t}{t_p}\right)^2\right] \tag{3}$$

where $R=0.6$ [18] is the target reflection coefficient, $t_p=100$ fs is the full-width at the half maximum (FWHM) with the linear polarization, $\alpha=14.2nm$ [18] is the penetration depth including the ballistic range, I is the incident laser fluence, $\beta=4\ln(2)$.

The temperature dependences of the electron heat capacity and electron-lattice coupling factor for noble metals are investigated based on the electron density of states (DOS) obtained from ab initio electronic structure calculations [19]. For Cu, at low electron temperatures, T_e~0.1 eV (~10^3 K), the region of the electron DOS affected by thermal excitations is similar to that of the free electron gas model, with only s electrons being excited. At higher electron temperatures, T_e~1 eV (~10^4 K), a significant number of d band electrons can be excited and can make a substantial contribution to the thermophysical properties of the material. The excitation of these electrons is expected to cause significant changes in the electron heat capacity and electron-lattice coupling factor. Therefore, the commonly used literature values of a linear temperature dependence of the C_e and a temperature independent constant value of G are inappropriate for the description of the strong irradiation regime. To account for this fact and to avoid an overestimation of electron temperatures, we have considered the nonlinear temperature dependences of C_e and G factors for copper as they are stated in Ref. [19]. In contrast, for the heat capacity of the copper lattice (C_l), the room-temperature value (3.5×10^6 J/m^3 K) is a reasonable approximation because it is known that the change in C_l upon temperature increase is very small [20].

The electron heat capacity is proportional to the electron temperature when the electron temperature is less than the Fermi temperature as $C_e=\gamma T_e$ [21] and $\gamma=\pi^2 n_e k_B/2T_F$, with $\gamma=96.6J/m^3K^2$ for Cu. n_e is the density of the free electrons, k_B is the Boltzmann's constant.

A relationship between the electron relaxation time and electron-electron scattering time $1/\tau_{e-e}=AT_e^2$ and electron-lattice scattering time $1/\tau_{e-l}=BT_l$ for electron temperatures below the Fermi temperature is given by $1/\tau=1/\tau_{e-e}+1/\tau_{e-l}=AT_e^2+BT_l$. The expression for the heat conductivity can be written as $k_e=k_{e0}BT_e/(AT_e^2+BT_l)$ [22], where k_{e0}, A and B are the material constants. As the electron temperature approaches and exceeds the Fermi temperature, the electron gas becomes nondegenerate and the electronic heat conductivity starts to increase with temperature. The high-temperature electron heat conductivity can be expressed as [18,22]

$$k_e=\chi\frac{\left(\mu_e^2+0.16\right)^{5/4}\left(\mu_e^2+0.44\right)\mu_e^2}{\left(\mu_e^2+0.092\right)^{1/2}\left(\mu_e^2+\eta\mu_l\right)} \tag{4}$$

Where $\mu_e=T_e/T_F$, $\mu_l=T_l/T_F$, and $T_F=8.12\times10^4$K which is the Fermi temperature of Cu. The parameters $\chi=377W/mK$ and $\eta=0.139$, which represent the material constants [18].

The electron temperature is very high under laser irradiation. It must consider the effect of the thermionic electron emission, is represented by the Richardson–Dushman equation [23]

$$J=\left(\frac{4\pi m}{h^3}\right)(k_BT_e)^2\exp\left[-\frac{e\varphi}{k_BT_e}\right] \tag{5}$$

where k_B is the Boltzmann constant, φ the work function of the metal, m is the mass of the electron and h is the Planck constant.

3. Experimental details

The laser system is a regenerative amplified Ti:Sapphire laser (Spectra Physics Tsunami oscillator and Spitfire amplifier). The full-width at the half maximum (FWHM) is 120 fs, the wavelength is 800 nm, the repetition rate is 1 kHz. The individual pulse is split into two sub-pulses by a beam splitter. The delay time may be changed from 1 to 110 ps. By a combination of a Glan laser polarizer and a half-wave plate, the energy of each sub-pulse can be attenuated to the desired value. The subpulses are directed by a beam splitter into a microscope objective (10×, NA=0.25), which focuses them onto the target material with a focal diameter of 3.6 μm and a Rayleigh range of 24 μm. We use a knife edge to measure the beam profile. The metal target is mounted on a computer-controlled X–Y–Z stage, which guarantees the sample location is new before each laser shot. All experiments are performed in air at atmospheric pressure. Each data point is an average of typically 20 shots. The fluctuation of the pulse-to-pulse spectral is less than 10%. The sample is positioned with its normal axis at an angle of 30° with respect to the laser beam direction. This structure can avoid the conflict between objective lens and collection lens. In the experiments, both pump pulses are s-polarized. Fluorescence perpendicular to the laser beam is collected by an f/2.0 lens, focused into a 0.25 m monochromator, and detected with a photomultiplier tube (PMT) [9].

4. Results and discussion

The double-pulse experimental results [9] are shown in Figs. 1 and 2. Fig. 1 displays the emission intensity obtained from a Cu sample with single pulse and double pulse. The laser fluence is 43 J/cm^2. The double-pulse delay time is 106 ps. The recorded spectrum of the double pulse is higher in intensity compared to the spectrum obtained with the single-pulse. Fig. 2(A) shows the emission intensity of the single-pulse and double pulse increased monotonically with the laser fluence. The emission line is the Cu (I) at 324.75 nm, produced by the [$3d^{10}4s(^2S_1)\leftarrow3d^{10}4p(^2P_{3/2})$] transition. In the experiment, the double-pulse delay time is fixed at 106 ps. Both curves are fitted with the polynomial, the enhancement ratio curve of the emission intensity of the double pulse to the single pulse is calculated by dividing the two fitting curves, as shown in Fig. 2(B). In the range of 0–4 J/cm^2, the enhancement ratio increases with the laser fluence. In this range, in Fig. 2(A), at values of the pulse energy close to the plasma threshold, the double-pulse arrangement results in a total density of Cu (I) that can be an order of magnitude higher than the density obtained following ablation with a single-pulse. This relative enhancement ratio, falls quickly as pulse energy is increased and

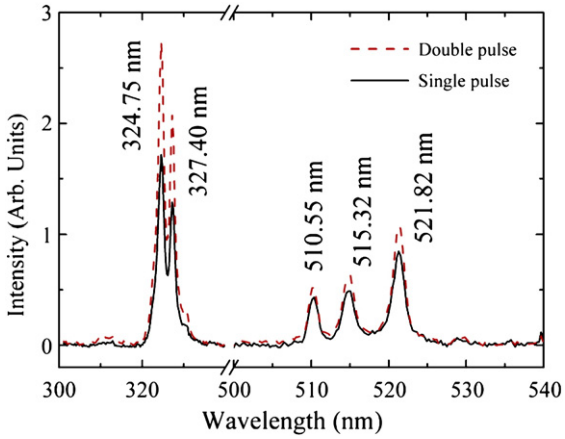

Fig. 1. The comparison of the emission intensity for Cu (I), corresponding to single-pulse (solid line) and double pulse (dash line). The laser fluence is 43 J/cm^2.

appears converging to a value around 2.5 at the high fluence range. For the fluence of 4 J/cm^2 and higher, the enhancement ratio monotonically decreases. The similar behavior for metal has been also noticed on the double-pulse laser-induced breakdown spectroscopy in the earlier experiment [6,24].

Several experimental and theoretical studies have been carried out to investigate the physical mechanisms involved in double-pulse laser–metal interactions. Despite significant progress in this field, the investigation of femtosecond double-pulse laser ablation remains a challenging research topic. In particular, the mechanisms of energy deposition and the processes the thermal diffusion are not yet fully understood. Next, we investigate the thermal behavior of femtosecond double-pulse laser heating Cu.

The time-dependence of the electron and lattice temperature on the surface of the target is represented in Fig. 3, which is predicted

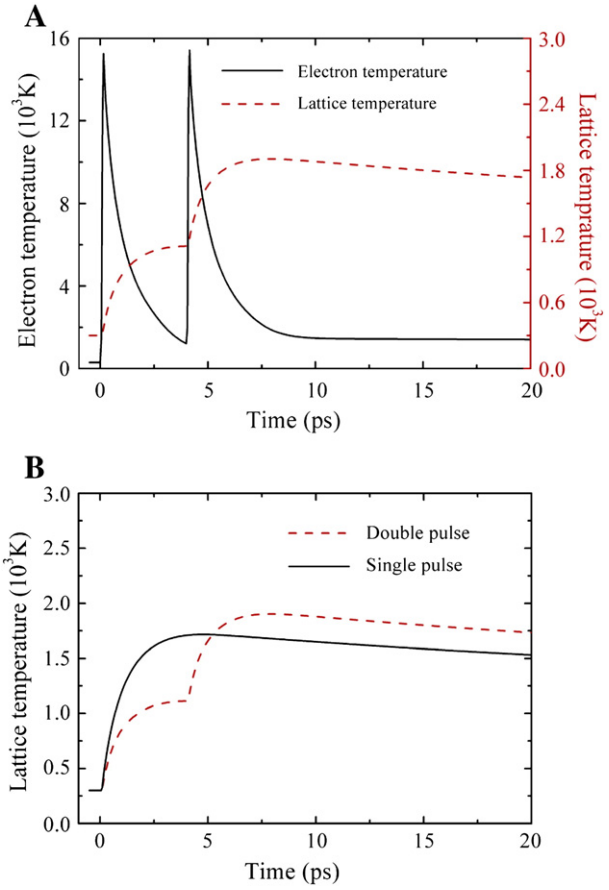

Fig. 3. The temperature variation with the delay time: (A) the electron and lattice temperature at the surface irradiated by the double-pulse laser; (B) the comparison of the lattice temperature under the single-pulse and double pulse. The whole laser fluence is 100 mJ/cm^2.

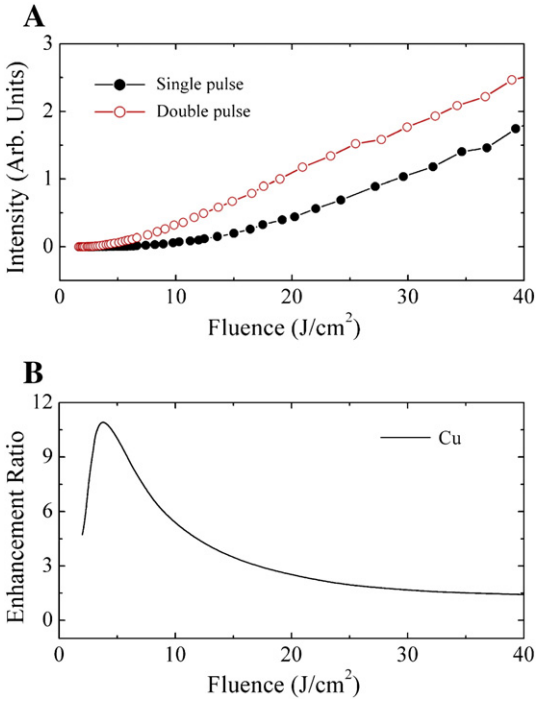

Fig. 2. (A) The emission intensity of the single-pulse and double pulse as a function of laser fluence. (B) The enhancement ratio as a function of laser fluence under the double pulse divided by the single-pulse. The emission line is the Cu (I) at 324.75 nm.

by the two-temperature model for the Cu target (100 nm). Fig. 3(A) shows the variation of the electron and lattice temperature at the different times by the femtosecond double-pulse laser, the laser fluence of each sub-pulse is 50 mJ/cm^2, the time interval of the double-pulse laser is 4 ps. Fig. 3(B) shows the comparison of the lattice temperature with the time. As can be seen, there is a very large difference in the evolution of the lattice temperature. In the single pulse case, the lattice temperature rapidly increases along with the delay time, and reaches the maximum value of 1716 K. Next, it slowly decreases when it, based on the heat transfer. However, in the case of the double-pulse laser, the lattice temperature firstly starts to increase and becomes very slow. Precisely at this time, the lattice temperature suddenly increases again, and reaches the maximum value of 1903 K. The time of the obtained maximum temperature is 4.7 ps and 7.9 ps, respectively. The double-pulse laser extends the thermal equilibrium time of the electron and lattice. Moreover, the lattice temperature has been achieved at a higher temperature relative to the single pulse case.

During the interaction of the double-pulse laser and metal, the delay time of two pulses is important to the maximum lattice temperature. The energy proportion of the first pulse to the second pulse is another concerned factor. Fig. 4 shows the contour map of the evolution of the maximum lattice temperature with the delay time of the double-pulse laser and the first pulse laser fluence (I_{first}), the second pulse laser fluence $I_{second} = I - I_{first}$. The whole fluences of Fig. 3(A) and (B) are 100 mJ/cm^2 and 200 mJ/cm^2, respectively. Seen from Fig. 4(A), for the delay times in 1–3 ps range, there are almost maximum lattice temperatures. For the first laser fluences, the maximum lattice temperatures may be achieved in 50–60 mJ/cm^2 range. So we

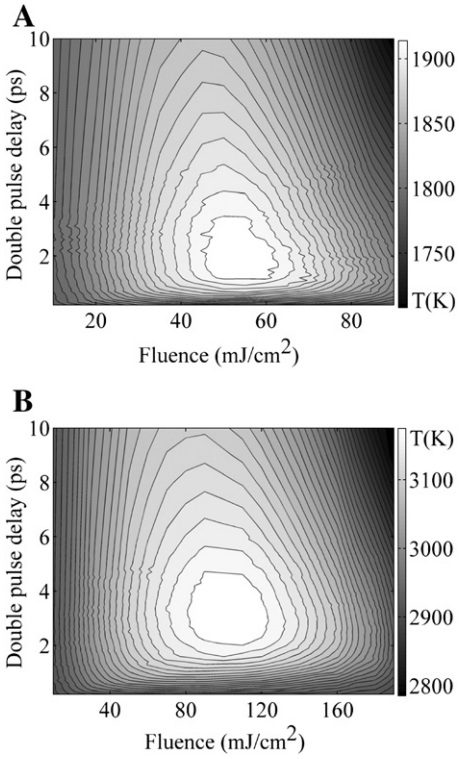

Fig. 4. The distribution of the maximum temperature with the double pulse delay and the first pulse fluence: (A) The whole laser fluence is 100 mJ/cm^2; (B) The whole laser fluence is 200 mJ/cm^2.

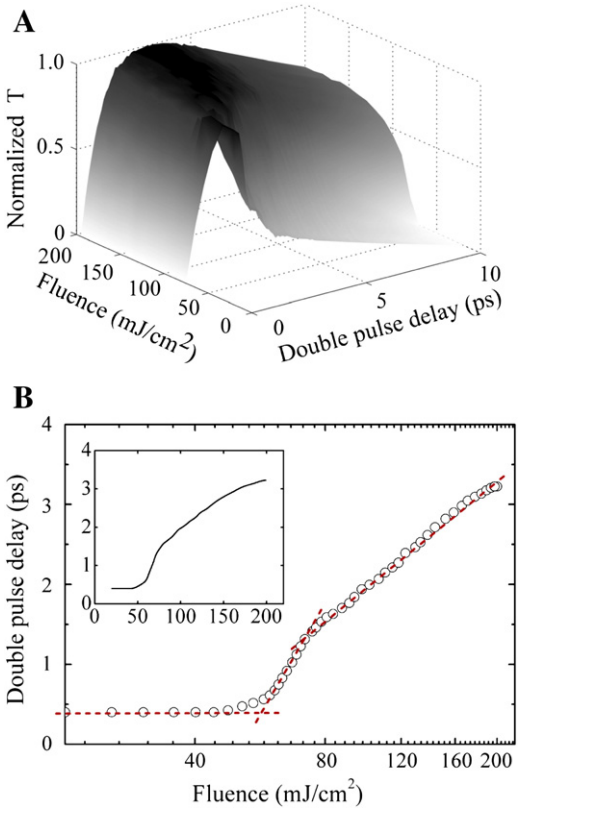

Fig. 5. (A) The normalized maximum lattice temperature as a function of the double-pulse delay and laser fluence. (B) The optimum double-pulse delay versus the fluence for obtaining the maximum temperature.

can obtain the maximum lattice temperature by attempting to change the proportion of first pulse to second pulse and the delay time of two pulses. A similar result is indicated in Fig. 4(B). One of both differences is an increase in the delay time of two pulses. Another one is the slight left-shift of the first laser fluence range. Further we confirm: the whole laser fluences have an obvious effect to the optimal double-pulse delay time for obtaining the maximum temperature, the effect of the proportion of first pulse to second pulse is very small at the different whole laser fluence.

In order to understand the details of the double-pulse temperature increase effect we will carry out a study of the influence of the whole laser fluence on the double-pulse delay time. Then the variation of the maximum lattice temperature with the whole laser fluence and the double-pulse delay is investigated. Fig. 5(A) shows the distribution of the normalized maximum lattice temperature. For obtaining the maximum temperature, the dependence of the double-pulse delay on the whole laser fluence is presented in Fig. 5(B). Three regions, i.e., three different logarithmic dependences, can be identified. In the low and intermediate fluence ranges a swift increase of the double-pulse delay was seen which levels out at approximately 50 mJ/cm^2. Continued to increase the whole laser fluence, it results in obviously increasing of the double-pulse delay. Till the laser fluence is about 80 mJ/cm^2, the delay time starts to become slow. Because of laser heating of metal film, the electron temperature becomes very high at the surface by absorbing laser energy, resulting in a very large change on the thermal physics properties, which play an important role in the processing of metallic targets under ultrashort laser pulses irradiation. In particular, the second pulse will act as an incubated energy resource continued to the thermal physics properties.

Fig. 6(A) shows the comparison of the maximum lattice temperature under the irradiation of the single pulse laser and the double pulse laser. In both cases, it has to be noted that the lattice temperature of single-pulse increases at a slower rate compared to double pulse with the increase of laser fluence. Moreover, the double-pulse lattice temperature is found to be higher by about 10–20% compared to the single-pulse case. In here, we assume that the lattice temperature (T_l) is proportional to the temperature of plasma T_p. At the local

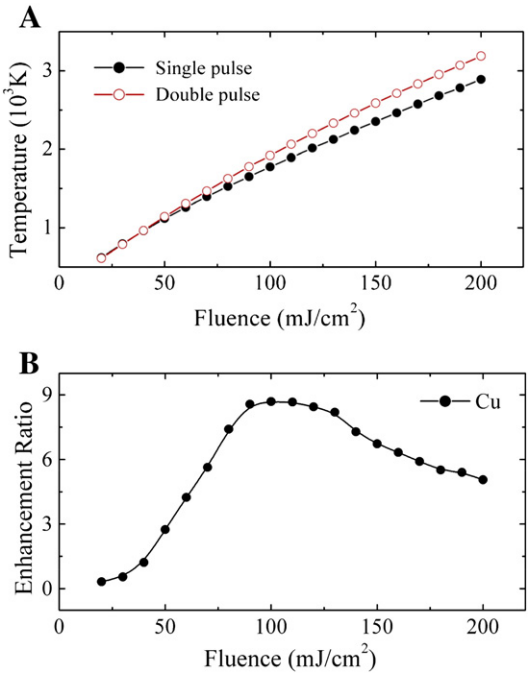

Fig. 6. (A) The maximum lattice temperature of the single-pulse and double pulse as a function of laser fluence. (B) The enhancement ratio as a function of laser fluence under the double pulse divided by the single-pulse.

thermodynamic equilibrium, the emission intensity of a spectroscopy, corresponding to a transition from level k to i, is given by [7]:

$$I_\lambda = F_{\exp} N \frac{A_{ki} g_k}{\lambda U(T_p)} \exp\left(-\frac{E_k}{k_b T_p}\right) \tag{8}$$

where A_{ki} is the transition probability, g_k and E_k are the degeneracy and energy of the upper level k, $U(T_p)$ is partition function, λ is the emission wavelength, k_b is Boltzmann constant, N is the total number density of a species in a given ionization stage, F_{exp} is the experimental coefficient with respect to the efficiency of the optical detection system. For the enhancement ratio of double-pulse emission intensity (I_{DP}) with respect to single-pulse emission intensity (I_{SP}), the expression can be simplified as:

$$\frac{I_{DP}}{I_{SP}} = a \exp\left(-b\left(\frac{1}{T_{DP}} - \frac{1}{T_{SP}}\right)\right) \tag{9}$$

$$\frac{I_{DP}}{I_{SP}} = a \exp\left(-bc\left(\frac{1}{T_{l-DP}} - \frac{1}{T_{l-SP}}\right)\right) \tag{10}$$

where T_{SP} and T_{DP} are the plasma temperatures of the single pulse and double pulse, $T_{l-SP} = c^* T_{SP}$ and $T_{l-DP} = c^* T_{DP}$ are the lattice temperatures of the single pulse and double pulse, a is experimental coefficient, $b = E_k/k_b$ is constant related to the wavelength, c is scale coefficient between lattice temperature and plasma temperature. Although a and c are not unknown in this study, it is still possible to use this equation in order to estimate an enhancement ratio. Fig. 6(B) shows the enhancement ratio as a function of the laser fluence in the single-pulse and double-pulse conditions. We see that at low fluence, with increasing fluence, the enhancement ratio also increases. When the laser fluence is around 100 mJ/cm^2, the ratio reaches the maximum value. Keep on increasing the laser fluence, the ratio starts to drop. We will see qualitatively a similar behavior on the experimental result in Fig. 2(B).

We note that restrictions of fluence may apply to these observations due to the experimental results against the simulation approach on Figs. 2 and 6. However we believe that the relative behavior remains valid. The lattice of metal will evolve into plasma after laser irradiation. The lattice temperature will have a certain proportion with the coming plasma temperature. The emission intensity of plasma will be related with the original lattice temperature. In here, on the expression (10), we can only provide the suppositive value of a and c, "coefficient a" may adjust the scale of "y axes", "coefficient c" may adjust the scale of "y axes" and the position of the maximum ratio. Using this method, the qualitative analysis can be done. We adjust the theoretical results (Fig. 6(B)) to the experimental results (Fig. 2(B)). The comparison can be shown in Fig. 7. The figure shows close agreement between the simulated and experimental data.

Several papers of the double-pulse laser-induced emission enhancement have analyzed the cause of the emission enhancement.

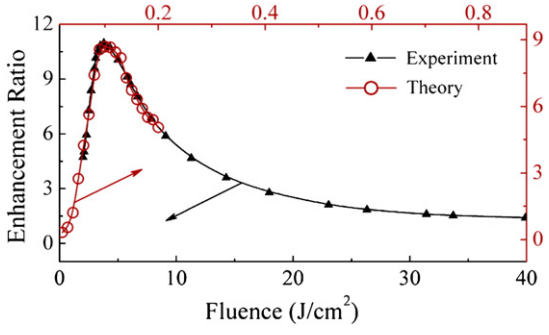

Fig. 7. The comparison of theoretical and experimental results for the enhancement ratio.

From a practical point of view, the process of the emission enhancement is very complex. This paper only uses a simple method to understand the mechanism of the emission enhancement. It is effective in realization of the double-pulse laser irradiation the metal target. However, the better emission enhancement mechanism has been not found for the double-pulse laser ablation in theory. Different combinations of laser beam geometries, wavelengths, pulse durations, and energies can be effectively used for optimum enhancement of emission from the double-pulse laser. The enhancement of the emission also depends on the properties of the target material and the ambient atmospheric conditions as well. This indicates that further investigation will provide even better results to explain the experimental observations.

5. Conclusions

In conclusion, a numerical solution of the two-temperature model has been performed up to the double-pulse femtosecond laser heated metal target at the low laser fluence. For the same total laser fluence, the lasers of single pulse and double pulse will lead to the different evolution of the electron and lattice temperature, and related thermophysical properties of the metal. The double-pulse laser will lead to higher lattice temperature and longer thermal relaxation time compared with the single-pulse laser. For obtaining the maximum lattice temperature, the increase of the double-pulse delay has two phases of logarithm changes on the laser fluences. Moreover, the computed results show that the enhancement ratio increases with laser fluence at the low fluence. However, for the higher fluence, the enhancement ratio decreases with laser fluence. Again, the experiment shows the similar change although not fully corresponding to the theoretical results. It illustrate that the calculated method needs further improvement.

Acknowledgements

This project was supported by the National Magnetic Confinement Fusion Science Program of China (grant no. 2010GB104003) and the National Natural Science Foundation of China (grant nos. 10974069, 10974070 and 11034003).

References

[1] A. Semerok, C. Dutouquet, Thin Solid Films 453–454 (2004) 501.
[2] S. Noël, J. Hermann, Applied Physics Letters 94 (2009) 053120.
[3] S. Amoruso, R. Bruzzese, X. Wang, Applied Physics Letters 95 (2009) 251501.
[4] S. Noël, E. Axente, J. Hermann, Applied Surface Science 255 (2009) 9738.
[5] S. Amoruso, R. Bruzzese, X. Wang, G. O'Connell, J.G. Lunney, Journal of Applied Physics 108 (2010) 113302.
[6] V. Piñon, D. Anglos, Spectrochimica Acta Part B 64 (2009) 950.
[7] V. Piñon, C. Fotakis, G. Nicolas, D. Anglos, Spectrochimica Acta Part B 63 (2008) 1006.
[8] Z. Hu, S. Singha, Y. Liu, R.J. Gordona, Applied Physics Letters 90 (2007) 131910.
[9] S. Singha, Z. Hu, R.J. Gordona, Journal of Applied Physics 104 (2008) 113520.
[10] S.I. Anisimov, B.L. Kapeliovich, T.L. Perel'man, Soviet Physics, JETP 39 (1974) 375.
[11] P.B. Corkum, F. Brunel, N.K. Sherman, T. Srinivasan-Rao, Physical Review Letters 61 (1988) 2886.
[12] A.M. Chen, H.F. Xu, Y.F. Jiang, D.J. Ding, L.Z. Sui, H. Liu, M.X. Jin, Applied Surface Science 257 (2010) 1678.
[13] A.M. Chen, Y.F. Jiang, L.Z. Sui, H. Liu, M.X. Jin, D.J. Ding, Journal of Optics 13 (2011) 055503.
[14] Z. Han, C. Zhou, E. Dai, J. Xie, Optics Communications 281 (2008) 4723.
[15] P.B. Allen, Physical Review Letters 59 (1987) 1460.
[16] J. Huang, Y.W. Zhang, J.K. Chen, Applied Physics A 95 (2009) (643 055503).
[17] W.Q. Hu, Y.C. Shin, G. King, Applied Physics A 98 (2010) 407.
[18] A.M. Chen, Y.F. Jiang, L.Z. Sui, D.J. Ding, H. Liu, M.X. Jin, Optics Communications 284 (2011) 2192.
[19] Z. Lin, L.V. Zhigilei, V. Celli, Physical Review B 77 (2008) 075133.
[20] D.R. Lide, Handbook of Chemistry Physics, 84th ed., CRC Press, Boca Raton, 2003, p. 12.
[21] J. Kim, S. Na, Optics & Laser Technology 39 (2007) 1443.
[22] G. Du, F. Chen, Q. Yang, J. Si, X. Hou, Optics Communications 283 (2010) 1869.
[23] S.S. Mao, X. Mao, R. Greif, R.E. Russo, Applied Physics Letters 73 (1998) 1331.
[24] M. Guillermin, A. Klini, J.P. Colombier, F. Garrelie, D. Gray, C. Liebig, E. Audouard, C. Fotakis, R. Stoian, Optics Express 18 (2010) 11159.